*Laser and Particle Beams* (2011), *29*, 279–282.

doi:10.1017/S0263034611000255

# Final compression beamline systems for heavy ion fusion drivers

Y.Y. LAU,[1] SIMON S. YU,[1,2] JOHN J. BARNARD,[3] AND PETER A. SEIDL[2]

[1]The Chinese University of Hong Kong, Shatin, Hong Kong
[2]Lawrence Berkeley National Laboratory, Berkeley, California
[3]Lawrence Livermore National Laboratory, Livermore, California

(Received 24 September 2009; Accepted 11 April 2011)

**Abstract**

We have identified a general final compression section for HIF drivers, the section between accelerator and the target. The beams are given a head to tail velocity tilt at the beginning of the section for longitudinal compression, while going through bends that direct it to the target at specific angle. The aim is to get the beams compressed while maintaining a small centroid off-set after the bends. We used a specific example, 1 MJ driver with 500 MeV Rubidium + 1 ion beams. We studied the effect of minimizing dispersion using different bend strategies, and came up with a beamline point design with adiabatic bends. We also identified some factors that lead to emittance growth as well as the minimum pulse length and spot size on the target.

**Keywords:** Drift compression; Heavy ion fusion; Momentum dispersion

## 1. INTRODUCTION

In current designs of heavy ion fusion drivers, manipulating multiple intense heavy ion beams is usually involved. For both direct and indirect drive, a drift compression section is needed between the accelerators and the fusion chamber, to direct the beams toward the target at specific geometry, and compress them at the same time for the short pulse lengths required for target ignition (De Hoon, 2001). It is shown that a simple four-polar-rings beam configuration around the target can achieve high uniformities with rotated beams (Runge & Logan, 2009). The benefit of this configuration can be maximized if the polar axis is aligned with the accelerators on both sides, and then only two designs of channels will be needed as the polar symmetry implies they will be nearly identical within the same group (Fig. 1). In general, the number of channel and target angles can vary depending on need, so the configuration works for any multiple beam direct or indirect drivers. We take the 1 MJ direct driver with 500 MeV Rb + 1 beams as an example.

Each beam channel consists of bends, a matching section, and a neutralized drift section (Roy *et al*., 2005). The beam is confined by a FODO lattice of quadrupole magnets, which also combines the function of bending dipoles. We use a constant focusing strength in this study (Grote *et al*., 2005), so as the beam compresses longitudinally, it expands transversely. There are two sets of bends in opposite directions (+x and –x), turning the beam by a total roughly 37°, which corresponds to one of the polar angle in the four-ring configuration. The beam then goes through the last four quads, which match the beam envelope to circular shape, into a plasma-filled neutralized drift section. It will get compressed down to the final length by the residual velocity tilt. A strong solenoid is placed at several meters away from the target for final focusing.

We used the three-dimensional particle-in-cell code WARP to simulate the beam in this study. The semi-Gaussian beam starts with a parabolic current profile and a matched envelope. The amount of initial velocity tilt, peak current, and pulse length are variable within ranges of the typical values. Table 1 show some parameters used in this study. Due to a relativity high beam perveance, a high velocity tilt is desirable for overcoming the space charge force and compressing the beam quickly. We choose a 10% tilt and a short drift length of roughly 100 m.

## 2. BEND STRATEGIES

As a result of the high velocity tilt, beam slices with different momentum travel orbits with various curvatures, which leads

Address correspondence and reprint requests to: Yuk Yeung Lau, The Chinese University of Hong Kong, Shatin, Hong Kong. E-mail: yylau@phy.cuhk.edu.hk

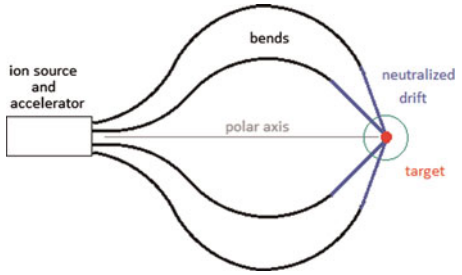


**Fig. 1.** (Color online) Overview of beam channels geometry. The opposite side (which is not shown here) is identical.

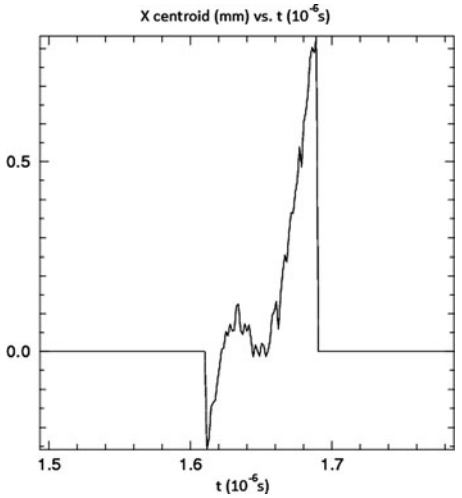


**Fig. 2.** Beam centroid of the whole beam as a function of t at bend end ($z = 55.5$ m) for adiabatic case. The maximum offset here is about 0.8 mm.

**Table 1.** *Parameters used in this study*

| Parameter | Value |
|---|---|
| Initial peak current/beam (A) | 100.0 |
| Energy/beam (kJ) | 7.5 |
| Initial perveance | $5.35 \times 10^{-5}$ |
| Initial pulse length, r.m.s. (ns) | 51 |
| Initial transverse emittance (π m rad) | $5.2 \times 10^{-5}$ |
| Initial longitudinal emittance (π m rad) | $4.56 \times 10^{-3}$ |
| Velocity tilt | −10% |
| Section total length (m) | ≈91 |
| Bend length (m) | 20, 30 |
| Neutralized drift length (m) | ≈27 |
| Lattice period (m) | 2.0 |
| Quad length (m) | 0.8 |
| Quad strength (T/m) | 64.33 |
| Max dipole strength (T) | 4.65 |
| Under-pressed tune (degree) | 72 |
| Pipe radius (cm) | 10 |

to beam dispersion. The short drift length will lead to sharper bends that impose further difficulties. In designing the bends, we take the idea in a previous paper, which showed that the centroid off-set can be kept at minimum by varying bend strength (Lee & Barnand, 2002). We adopted similar bend strategies, namely abrupt bend, matched bend, and adiabatic bend. However, due to the limited drift length for the adiabatic bend, instead of varying bend strength slowly over several (under-pressed) betatron periods, we used a linear ramp of one betatron period for both up and down. Also all the bend lengths are integral multiples of the betatron period for the best chromaticity. The dipole strength of each strategy is shown as follow (Table 2).

Figures 2 and 3 shows the evolution of centroid off-set for an off-momentum slice of the beam. The maximum off-sets of the beam tips at end of the bend ($z = 55.5$ m) are 3.4 mm, 1.3 mm, and 0.8 mm, respectively, for the three bend cases. It is clear that an adiabatic or a matched design result in significant lower off-set then an abrupt design. The drawback is they require stronger dipole field.

## 3. NEUTRALIZED DRIFT SECTION AND FINAL FOCUS

The straight section after the bends is the neutralized drift section, in which the space charge force is assumed to be completely gone in the simulations. It starts at $z = 64.6$ m and there is roughly 27 m away from the longitudinal focus for an approximately 6.5% residual tilt. Within this region, the beam is allowed to expand transversely by a slight angle generated by the matching quads; this is desirable for the final spot size. With a 12 T solenoid at 4 m away, we get a 5 mm spot, 0.08 m (2.4 ns) pulse length at $z = 91$ m (Figs. 4 and 5).

As a result of no space charge, the final spot and pulse length will depend mainly on the emittances in the corresponding directions. To look at this effect, we repeat the simulations with reduced initial emittances in both directions. Which are 1/2, 1/4 of the first run values, and last with zero emittances. Emittances in the two directions are defined respectively as:

$$\varepsilon_x = 4\sqrt{\langle(\Delta x)^2\rangle\langle(\Delta x')^2\rangle - \langle \Delta x\ \Delta x'\rangle^2}, \quad (1)$$

$$\varepsilon_z = \frac{4}{\langle v_z\rangle}\sqrt{\langle(\Delta z)^2\rangle\langle(\Delta v_z)^2\rangle - \langle \Delta z\ \Delta v_z\rangle^2}, \quad (2)$$

where $\Delta x = x - \langle x\rangle$ and all similar quantities are the deriviation from the mean and $\langle\ \rangle$ denotes average over particles.

Tables 3 and 4 shows the results with different initial emittances. The final pulse length and current are typical requirement values for HIF drivers. However, we did not get a small

**Table 2.** *Dipole strength associated with each bend strategy*

| Design | First arc values (T) | Second arc values (T) |
|---|---|---|
| Abrupt bend | 2.38 | 2.38 |
| Matched bend | 1.69, 3.38 | 1.49, 2.98 |
| Adiabatic bend | Max 4.65 | Max 3.57 |

https://doi.org/10.1017/S0263034611000255 Published online by Cambridge University Press

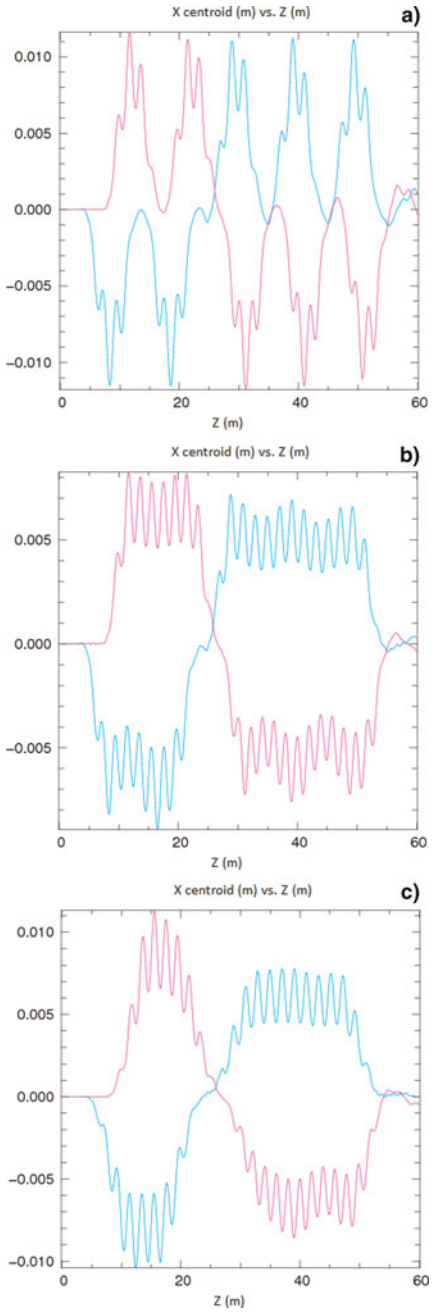


**Fig. 3.** (Color online) Beam centroid as a function of z for the case: (**a**) abrupt bend, (**b**) matched bend, and (**c**) adiabatic bend, for two slices halfway to the beam head and tail, respectively.

spot even with the smallest possible transverse emittance, and a reasonable maximum final converging angle, limited by the pipe radius, solenoid strength, and size of the fusion chamber. The spot size is partly due to chromatic effect, as a result of the residual velocity tilt, the beam head and tail have different focal lengths (Fig. 6). It is clear that even in this case, the spot is dominated by emittance.

We take the case with small initial values (Case 3 in the above) as an example to illustrate the fundamental emittance limit. Figure 7 shows $\varepsilon_x$, $\varepsilon_y$, and $\varepsilon_z$ *vs.* $z$, we observe the

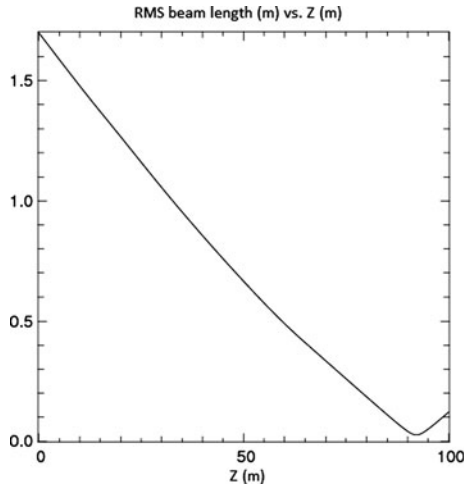


**Fig. 4.** Beam length as a function of $z$.

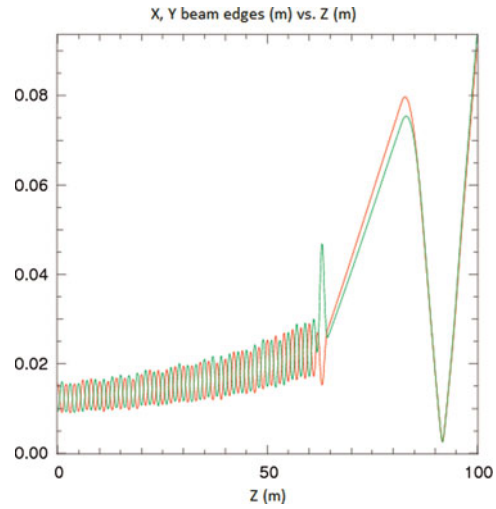


**Fig. 5.** (Color online) Beam edges as function of $z$, red line is $x$ and green line is $y$, respectively.

**Table 3.** *Spot sizes with different initial $\varepsilon_x$ values*

| Initial $\varepsilon_x$ ($10^{-5}\pi$ m rad) | Spot size (mm) | Central slice spot (mm) |
|---|---|---|
| 5.2 | 5.6 | 5.2 |
| 2.6 | 4.2 | 4.0 |
| 1.3 | 3.0 | 2.8 |
| 0.0 | 2.6 | 2.1 |

following: (1) $\varepsilon_z$ grows steadily with the distance traveled in vacuum section but remains constant in neutralized section, so it is believed that $\varepsilon_z$ growth is only due to space charge force. (2) $\varepsilon_x$ is affected by the bends as there are clear rises at the locations. (3) $\varepsilon_x$ and $\varepsilon_y$ tends to equilibrate as seen from the region before the neutralization, still $\varepsilon_x$ ends up larger than $\varepsilon_y$. The value at the focus is about

https://doi.org/10.1017/S0263034611000255 Published online by Cambridge University Press

**Table 4.** *Final pulse length and final peak current with different initial $\varepsilon_z$, note that the longitudinal focus occurs at slightly further away with lower $\varepsilon_z$*

| Initial $\varepsilon_z$ ($10^{-3}\pi$ m rad) | Final rms length (ns) | Final current (A) |
|---|---|---|
| 4.56 | 2.26 | 2050 |
| 2.28 | 1.34 | 3900 |
| 1.14 | 0.83 | 7000 |
| 0.00 | 0.60 | 12200 |

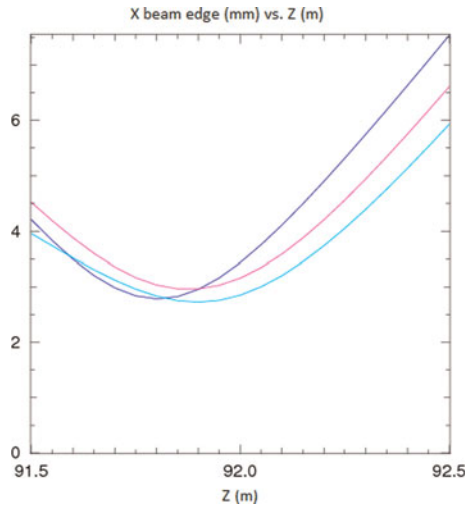


**Fig. 6.** (Color online) Beam edge as function of $z$ near the focus for the case with low initial emittances, blue line corresponds to central slice; purple and cyan lines are off momentum slices near the beam tail and head, respectively.

$3 \times 10^{-5}$ π m rad. More detailed analysis on factors affecting emittance growth will be made in future works.

## 4. CONCLUSIONS

We have proposed here a general strategy to layout the final compression beamline for any multiple beam direct and indirect drivers, which utilize the symmetry to simplify the design of individual beam channels. We have also shown some key features using an example of a relatively low energy, high perveance beam with parameters compatible with a full driver system. The adiabatic bend design used in this study works well, even with a relativity high velocity tilt and short drift length.

We observed emittance growth in the section that will place constraints on the final spot size and pulse length on the target. Particularly in the example studied, more advanced, and carefully designed focusing schemes may be necessary to compress the spot sizes to meet target requirements. Some mechanisms for emittance growth and the parametric dependence are being investigated; the results will be published elsewhere.

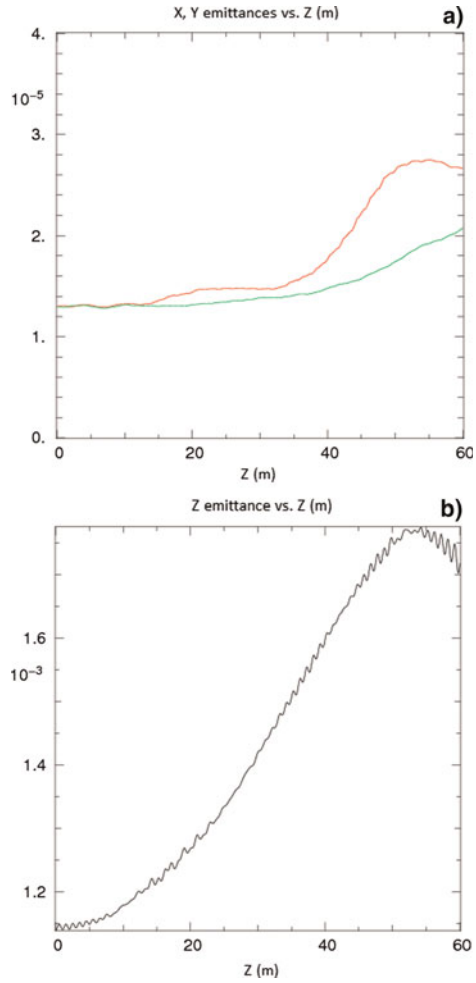


**Fig. 7.** (Color online) (**a**) $\varepsilon_x$ (red line) and $\varepsilon_y$ (green line) of beam central slice *vs.* $z$ and (**b**) $\varepsilon_z$ of the whole beam *vs.* $z$.

## REFERENCES

De Hoon, M.J.L. (2001). *Drift Compression and Final Focus Systems for Heavy Ion Inertial Fusion*. Ph.D. Thesis, University of California, Berkeley.

Grote, D.P., Friedman, A., Vay, J.L. & Haber, I. (2005). The WARP code: Modeling high intensity ion beams. *AIP Conf. Proc*. **749**, 55–58.

Lee, E.P. & Barnard, J.J. (2002). Bends and momentum dispersion during final compression in heavy ion fusion drivers. *Laser Part. Beams* **20**, 581–584.

Roy, P.K., Yu, S.S., Henestroza, E., Anders, A., Bieniosek, F.M., Coleman, J., Eylon, S., Greenway, W.G., Leitner, M., Logan, B.G., Waldon, W.L., Welch, D.R., Thoma, C., Sefkow, A.B., Gilson, E.P., Efthimion, P.C. & Davidson, R.C. (2005). Drift compression of an intense neutralized ion beam. *Phys. Rev. Lett*. **95**, 234801.

Runge, J. & Logan, B.G. (2009). Nonuniformity for rotated beam illumination in directly driven heavy-ion fusion. *Phys. Plasmas* **16**, 033109.

https://doi.org/10.1017/S0263034611000255 Published online by Cambridge University Press